
KG-GAN: Knowledge-Guided Generative Adversarial Networks

Che-Han Chang¹, Chun-Hsien Yu¹, Szu-Ying Chen¹, and Edward Y. Chang^{1,2}

¹HTC Research & Healthcare

²Stanford University

{chehan_chang, jimmy_yu, claire.sy_chen, edward_chang}@htc.com

Abstract

Generative adversarial networks (GANs) learn to mimic training data that represents the underlying true data distribution. However, GANs suffer when the training data lacks quantity or diversity and therefore cannot represent the underlying distribution well. To improve the performance of GANs trained on under-represented training data distributions, this paper proposes KG-GAN to fuse domain knowledge with the GAN framework. KG-GAN trains two generators; one learns from data while the other learns from knowledge. To achieve KG-GAN, domain knowledge is formulated as a constraint function to guide the learning of the second generator. We validate our framework on two tasks: fine-grained image generation and hair recoloring. Experimental results demonstrate the effectiveness of KG-GAN.

1 Introduction

Generative adversarial networks (GANs) [1] and their variants have received massive attention in the machine learning and computer vision communities recently due to their impressive performance in various tasks, such as categorical image generation [2], text-to-image synthesis [3] [4], image-to-image translation [5] [6] [7], and semantic manipulation [8]. The goal of GANs or e.g., cGANs is to learn a generator that mimics the underlying distribution represented by a finite set of training data. Considerable progress has been made to improve the robustness of GANs.

However, when the training data does not represent the underlying distribution well, i.e., the empirical training distribution deviates from the underlying distribution, GANs trained from under-represented training data mimic the training distribution, but not the underlying one. This situation occurs because data collection is labor intensive and it is difficult to be thorough. Additionally, some modes of the underlying distribution could be missing in the training data due to insufficient quantity and in particular, diversity. Specifically, we consider that the underlying distribution is under-represented by the training data *at the category level*, i.e., some categories have no training data examples.

Training a GAN conditioned on category labels requires collecting training examples for each category. If some categories are not available in the training data, then it appears infeasible to learn to generate their representations without any additional information. For instance, in the task of hair recoloring (or hair color transfer), if we want to train an image-to-image translation model that recolors hair by rare colors such as purple, it is necessary to collect images with those hair colors. However, it is impractical to collect all possible dyed hair colors for arbitrary recoloring. Another example is that if the training data consists of only red colored roses, the GANs' discriminators would reject the other colors of roses and fail to generate roses of colors other than red. At the same time, we want to ensure that GANs will not generate a rose with an unnatural color. To the best of our knowledge, no previous works have investigated improving the diversity of the training distribution to better mimic the underlying distribution.

To this end, we propose Knowledge-Guided Generative Adversarial Networks (KG-GANs), a novel GAN framework that incorporates *domain knowledge* into GANs to enrich and expand the generated distribution, hence increasing the diversity of the generated data at the category level. Our key idea is

to leverage domain knowledge as another learning source other than data to guide the generator to explore different regions of the image manifold. By doing so, the generated distribution goes beyond the training distribution and better mimics the underlying one. Note that domain knowledge serves GANs as a guide not only to explore diversity but also to constrain exploring into regions that are knowingly impossible, such as generating gray roses.

Our framework consists of two parts: (1) constructing the domain-knowledge for the task at hand, and (2) training two generators G_1 and G_2 that are conditioned on available and unavailable categories, respectively. We formalize domain-knowledge as a constraint function that explicitly measures whether an image has the desired characteristics of a particular category. On the one hand, the constraint function is task-specific and guides the learning of G_2 . On the other hand, we share weights between G_1 and G_2 to leverage the knowledge learned from available to unavailable categories.

We validate KG-GAN on two tasks: fine-grained image generation and hair recoloring. For fine-grained image generation, such as flower images with different species, we aim to train a category-conditional generator that is capable of generating both seen and unseen categories. The domain knowledge we use here is a semantic embedding representation that describes the semantic relationships among fine-grained categories, such as the textual features from descriptions of each category’s appearance. The constraint function used is a deep regression network that predicts the semantic embedding vector of the underlying category of an image.

For hair recoloring, given the training data consists of three hair colors, our method trains an image-to-image translation model that is capable of recoloring face images with *arbitrary* hair colors. We leverage the domain knowledge that hair color is characterized by the dominant color of the hair region (not including eyebrows and beard). In this case, hair segmentation plays a key role in implementing the constraint function that performs hair color estimation. We jointly train the segmentation network, G_1 , and G_2 in an unsupervised manner. We additionally leverage the observation that hair recoloring can be safely assumed as a spatially invariant linear transformation applied only on the hair region. We propose a new generator architecture that outputs transformations rather than images. This significantly improves the segmentation accuracy and hence the recoloring quality.

Our main contributions are summarized as follows: (1) We tackle the problem that the training data cannot well represent the underlying distribution. (2) We propose a novel generative adversarial framework that incorporates domain knowledge into GAN methods. (3) We demonstrate the effectiveness of our KG-GAN framework on fine-grained image generation and hair recoloring tasks. We are able to enrich the diversity of the generated distribution by generating categories not available in the original training data.

2 Related work

Since a comprehensive review of the related works on GANs is beyond the scope of the paper, we only review representative works most related to ours.

Generative Adversarial Networks. Generative adversarial networks (GANs) [1] introduce an adversarial learning framework that jointly learns a discriminator and a generator to mimic a training distribution. Conditional GANs (cGANs) extend GANs by conditioning on additional information such as category label [9, 2], text [3], or image [5, 6, 7]. SN-GAN [2, 10] proposes a projection discriminator and a spectral normalization method to improve the robustness of training. CycleGAN [6] employs a cycle-consistency loss to regularize the generator for unpaired image-to-image translation. StarGAN [7] proposes an attribute-classification-based method that adopts a single generator for multi-domain image-to-image translation. Hu et al. [11] introduce a general framework that incorporates domain knowledge into deep generative models. Its primary purpose is improving quality, but not improving diversity, which is our goal.

Diversity. Creative adversarial network (CAN) [12] augments GAN with two style-based losses to make its generator go beyond the training distribution and thus generate diversified art images. Imaginative adversarial network (IAN) [13] proposes a two-stage generator that goes beyond a source domain (human face) and towards a target domain (animal face). Both works aim to go beyond the training data. However, they target art image generation and do not possess a well-defined underlying distribution. Mode-Seeking GAN [14] proposes a mode seeking regularization method to alleviate the mode collapse problem in cGANs, which happens when the generated distribution cannot well represent the training distribution. Our problem appears similar but is ultimately different. We tackle the problem that the training distribution under-represents the underlying distribution.

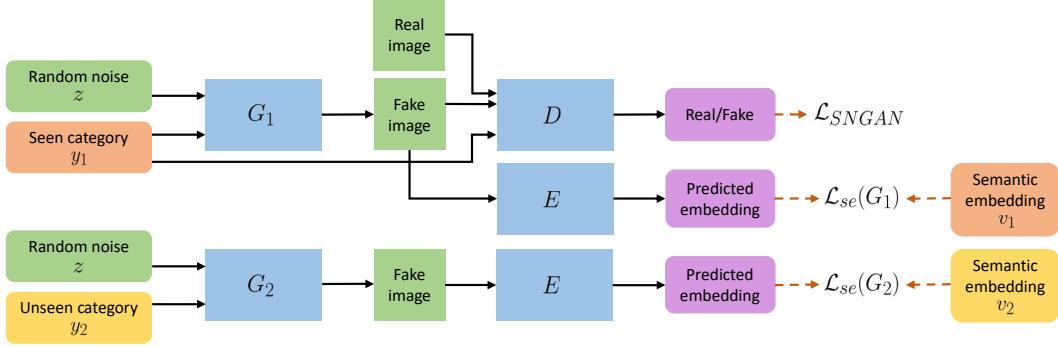


Figure 1: The schematic diagram of KG-GAN for fine-grained image generation. There are two generators G_1 and G_2 , a discriminator D , and an embedding regression network E as the constraint function. We share all the weights between G_1 and G_2 . By doing so, our method here can be treated as training a single generator with a category-dependent loss that seen and unseen categories correspond to optimizing two losses (\mathcal{L}_{SNGAN} and \mathcal{L}_{se}) and a single loss (\mathcal{L}_{se}), respectively, where \mathcal{L}_{se} is the semantic embedding loss.

Zero-shot Learning We refer readers to [15] for a comprehensive introduction and evaluation of representative zero-shot learning methods. The crucial difference between their and our method is that they focus on image classification while we focus on image generation. Recently, some zero-shot methods [16, 17, 18] propose to learn feature generation of unseen categories for training zero-shot classifiers. Instead, this work aims to learn image generation of unseen categories.

3 KG-GAN

This section presents our proposed KG-GAN that incorporates domain knowledge into the GAN framework. We first provide an overview of KG-GAN. Then, we show how to apply KG-GAN on two representative tasks: fine-grained image generation and hair recoloring.

We consider a set of training data under-represented at the category level, i.e., all training samples belong to the set of seen categories, denoted as Y_1 (e.g., black, brown, blond hair color categories), while another set of unseen categories, denoted as Y_2 (e.g., any other hair color categories), has no training samples. Our goal is to learn categorical image generation for both Y_1 and Y_2 . To generate new data in Y_1 , KG-GAN applies an existing GAN-based method to train a category-conditioned generator G_1 by minimizing GAN loss \mathcal{L}_{GAN} over G_1 . To generate unseen categories Y_2 , KG-GAN trains another generator G_2 from the domain knowledge, which is expressed by a constraint function f that explicitly measures whether an image has the desired characteristics of a particular category.

KG-GAN consists of two parts: (1) constructing the domain knowledge for the task at hand, and (2) training two generators G_1 and G_2 that condition on available and unavailable categories, respectively. KG-GAN shares the parameters between G_1 and G_2 to couple them together and to transfer knowledge learned from G_1 to G_2 . Based on the constraint function f , KG-GAN adds a *knowledge loss*, denoted as \mathcal{L}_K , to train G_2 . The general objective function of KG-GAN is written as $\min_{G_1, G_2} \mathcal{L}_{GAN}(G_1) + \lambda \mathcal{L}_K(G_2)$.

3.1 Fine-grained Image Generation

Given a fine-grained image dataset that some categories are unseen, our aim is using KG-GAN to generate unseen categories in addition to the seen categories. Figure 1 shows an overview of KG-GAN for fine-grained image generation. Our generators take a random noise z and a category variable y as inputs and generate an output image x' . In particular, $G_1 : (z, y_1) \mapsto x'_1$ and $G_2 : (z, y_2) \mapsto x'_2$, where y_1 and y_2 belong to the set of seen and unseen categories, respectively.

We leverage the domain knowledge that fine-grained categories are characterized by a semantic embedding representation, which describes the semantic relationships among categories. In other words, we assume that each category is associated with a semantic embedding vector v . For example, we can acquire such feature representation from the textual descriptions of each category. We propose the use of the semantic embedding in two places. One is for modifying the GAN architecture, and the other is for defining the constraint function.

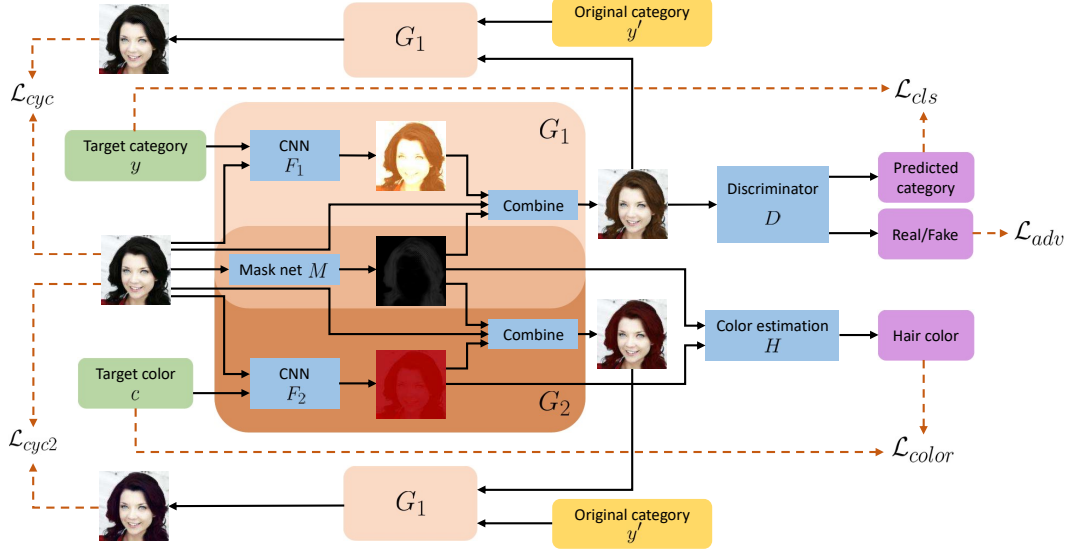


Figure 2: The schematic diagram of KG-GAN for hair recoloring. There are two generators G_1 and G_2 , a discriminator $D = \{D_{src}, D_{cls}\}$, and a segmentation-based color estimation network H as the constraint function. G_1 learns categorical recoloring from the training data by optimizing the StarGAN loss comprised of \mathcal{L}_{adv} , \mathcal{L}_{cls} , and \mathcal{L}_{cyc} . G_2 learns arbitrary recoloring from domain knowledge by minimizing the color loss \mathcal{L}_{color} and the cycle loss \mathcal{L}_{cyc2} . To achieve transferring the knowledge learned from G_1 to G_2 , we share the mask network M and partial weights between F_1 and F_2 . Please see the supplementary material for the details of our transform generator.

SN-GAN. Here we briefly review SN-GAN (please refer to [2, 10] for more details), which is adopted as the GAN part of KG-GAN. SN-GAN employs a projection-based discriminator D and adopts spectral normalization for discriminator regularization. The objective functions for training G_1 and D use a hinge version of adversarial loss. The category variable y_1 in SN-GAN is a one-hot vector indicating which target category. We propose to replace the one-hot vector by the semantic embedding vector v_1 . By doing so, we directly encode the domain knowledge into the GAN training. The loss functions of the modified SN-GAN are defined as

$$\begin{aligned} \mathcal{L}_{SNGAN}^G(G_1) &= -\mathbb{E}_{z, v_1} [D(G_1(z, v_1), v_1)], \text{ and} \\ \mathcal{L}_{SNGAN}^D(D) &= \mathbb{E}_{x, v_1} [\max(0, 1 - D(x, v_1))] + \mathbb{E}_{z, v_1} [\max(0, 1 + D(G_1(z, v_1), v_1))]. \end{aligned} \quad (1)$$

Semantic Embedding Loss. We define the constraint function f as predicting the semantic embedding vector of the underlying category of an image. To achieve that, we implement f by training an embedding regression network E from the training data. Once trained, we fix its parameters and add it to the training of G_1 and G_2 . In particular, we propose a semantic embedding loss \mathcal{L}_{se} as the role of knowledge loss in KG-GAN. This loss requires the predicted embedding of fake images to be close to the semantic embedding of target categories. \mathcal{L}_{se} is written as

$$\mathcal{L}_{se}(G_i) = \mathbb{E}_{z, v_i} \|E(G_i(z, v_i)) - v_i\|^2, \text{ where } i \in \{1, 2\}. \quad (2)$$

Total Loss. The total loss is a weighted combination of \mathcal{L}_{SNGAN} and \mathcal{L}_{se} . The loss functions for training D and for training G_1 and G_2 are respectively defined as

$$\begin{aligned} \mathcal{L}^D &= \mathcal{L}_{SNGAN}^D(D), \text{ and} \\ \mathcal{L}^G &= \mathcal{L}_{SNGAN}^G(G_1) + \lambda_{se}(\mathcal{L}_{se}(G_1) + \mathcal{L}_{se}(G_2)). \end{aligned} \quad (3)$$

3.2 Hair Recoloring

Given a set of face images categorized by hair color, which is defined as a discrete set Y_1 of representative colors. (For example, $Y_1 = \{\text{black, brown, blond}\}$ in the CelebA dataset [19].) Our goal is using KG-GAN to achieve hair recoloring with arbitrary colors. Figure 2 shows an overview. Given an input face image x , hair recoloring aims to transfer the image's hair color into a target color

c. Here, KG-GAN trains $G_1 : (x, y) \mapsto x'_1$ and $G_2 : (x, c) \mapsto x'_2$ where $y \in Y_1$ is the target category represented by a one-hot vector, and c is the target color represented by a 3D RGB vector.

To train G_1 , we adopt StarGAN [7] as the GAN part of our KG-GAN. For G_2 , we leverage two pieces of domain knowledge about hair color: (1) hair color is characterized by the dominant color of the hair region (the upper part of head), and (2) if the hair region can be identified, its recoloring process can be simplified as a simple color transfer. We use the former domain knowledge for defining the constraint function while the latter is used for designing a specialized generator architecture.

StarGAN. Here we briefly review StarGAN. Please refer to [7] for more details. StarGAN learns a single generator to perform multi-domain image-to-image translation. In our case, we can train a StarGAN model on the CelebA Face Dataset to translate images into one of the three categories (i.e., domains): black, brown, and blond. The StarGAN discriminator $D = \{D_{src}, D_{cls}\}$ performs domain classification and discrimination between real and fake images, i.e., $D : x \mapsto \{D_{src}(x), D_{cls}(x)\}$.

The total loss in StarGAN is comprised of three losses: an adversarial loss \mathcal{L}_{adv} , a domain classification loss \mathcal{L}_{cls} , and a cycle-consistency loss \mathcal{L}_{cyc} . The adversarial loss \mathcal{L}_{adv} is a W-GAN loss [20] with a gradient penalty term [21]. The domain classification loss \mathcal{L}_{cls} is responsible for translation quality. The cycle-consistency loss \mathcal{L}_{cyc} regularizes the generator. The loss functions used in training D and G_1 are respectively defined as

$$\begin{aligned}\mathcal{L}_{StarGAN}^D &= \mathcal{L}_{adv}^D + \lambda_{cls} \mathcal{L}_{cls}^r, \text{ and} \\ \mathcal{L}_{StarGAN}^G &= \mathcal{L}_{adv}^G + \lambda_{cls} \mathcal{L}_{cls}^f + \lambda_{cyc} \mathcal{L}_{cyc}.\end{aligned}\tag{4}$$

Hair Color Estimation. Hair color is characterized by the dominant color of the hair region. Therefore, we define the constraint function f as explicitly extracting the hair color from an image. To this end, we propose a segmentation-based color estimation network H that consists of two steps: (1) Performing hair segmentation to obtain the hair probability map s of the input image x . (2) A weighted average of x weighted by s to obtain the hair color, which is expressed by

$$H(x) = \frac{\sum_i w(s_i) x_i}{\sum_i w(s_i)},\tag{5}$$

where s_i and x_i are the i -th pixel value of s and x , respectively. w is a weighting function that turns the segmentation probabilities into binary weights. w is defined as $w(s_i) = \mathbb{I}[s_i > 0.5 \max_j(s_j)]$ where \mathbb{I} is the indicator function.

Hair Segmentation. The first step of H requires hair segmentation. Instead of training the hair segmentation sub-network S from another set of labeled training data, we propose training S in an unsupervised manner by jointly training G_1 , G_2 , and S together. Following recent image-to-image translation methods [22, 23] that adopt mask mechanism in their generator architecture, we add a mask network M in the StarGAN generator and shares its parameters with the segmentation sub-network S in H . On the one hand, the modified StarGAN generator performs image translation by $G_1(x, y) = M(x) \otimes F_1(x, y) + (1 - M(x)) \otimes x$, where $M(x)$ is a mask image, \otimes is pixel-wise multiplication, and F_1 is a convolutional neural network that generates the foreground image. On the other hand, hair segmentation is learned *from* training G_1 and is utilized in the color estimation network H for training G_2 .

Generator Architecture. Since hair segmentation plays an essential role in the constraint function, its accuracy directly influences the quality of G_2 . However, the masks from the modified StarGAN generator do not guarantee to localize hair region. It is because an inaccurate hair mask could still yield a high-quality result as long as $F_1(x, y)$ is of high-quality.

To further improve the accuracy of unsupervised segmentation, we leverage domain knowledge: if we can identify the hair region, we can simplify the recoloring process as a simple color transfer. Specifically, we assume the recoloring process is a spatially invariant linear transformation. Such an assumption greatly restricts the foreground generation from a highly nonlinear mapping to a linear one. By doing so, the segmentation network is forced to be more accurate; otherwise, a false-positive region (such as eyebrows) could be transformed into an unrealistic color and then appears in the output image. The linear transformation, parameterized by a 3×4 matrix $[w|b]$, takes a pixel color x_i as input and outputs a new color x'_i by $x'_i = wx_i + b$. Such a transformation can be equivalently expressed by a 1×1 convolution as $\text{conv}_{1 \times 1}(x; [w|b])$. Finally, based on M and $\text{conv}_{1 \times 1}$,

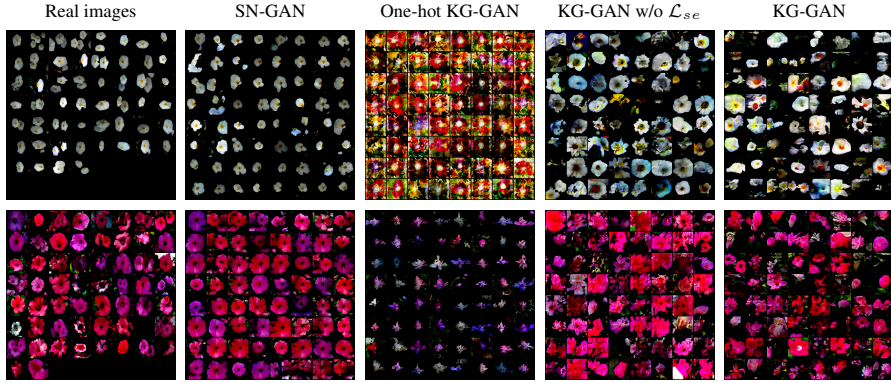


Figure 3: **Fine-grained image generation.** Qualitative comparison between real images, SN-GAN, and KG-GAN. These two flower categories (Orange Dahlia and Stemless Gentian) are seen to SN-GAN while unseen to KG-GAN.

our *transform generators* G_1 and G_2 are respectively defined as

$$\begin{aligned}
 y_1 &= G_1(x, y) = M(x) \otimes F_1(x, y) + (1 - M(x)) \otimes x \\
 &= M(x) \otimes \text{conv}_{1 \times 1}(x; T_1(x, y)) + (1 - M(x)) \otimes x, \text{ and} \\
 y_2 &= G_2(x, c) = M(x) \otimes F_2(x, c) + (1 - M(x)) \otimes x \\
 &= M(x) \otimes \text{conv}_{1 \times 1}(x; T_2(x, c)) + (1 - M(x)) \otimes x,
 \end{aligned} \tag{6}$$

where $T_1(x, y)$ and $T_2(x, c)$ are convolutional neural networks that generate 1×1 convolutional filters.

Color Loss. Based on Equation 5, We propose a color loss \mathcal{L}_C as the knowledge loss in KG-GAN. \mathcal{L}_C encourages the predicted color of the foreground image, $\text{conv}_{1 \times 1}(x; T_2(x, c))$, to be close to the target color c , which is uniformly sampled from the RGB color space. The color loss is written as

$$\mathcal{L}_{color} = \mathbb{E}_{x,c} \|\text{conv}_{1 \times 1}(x; T_2(x, c)) - c\|_1. \tag{7}$$

Cycle Loss. In addition to the cycle-consistency loss \mathcal{L}_{cyc} in StarGAN for regularizing G_1 , we propose another cycle-consistency loss \mathcal{L}_{cyc2} that considers both G_1 and G_2 to further improve G_2 with the aid of G_1 . In particular, x is first transferred through G_2 to become $G_2(x, c)$ and then transfers back to the original category l' through G_1 . \mathcal{L}_{cyc2} is defined accordingly as

$$\mathcal{L}_{cyc2} = \mathbb{E}_{x,c,y'} [\|G_1(G_2(x, c), y') - x\|_1]. \tag{8}$$

Total loss. The total loss is a weighted combination of $\mathcal{L}_{StarGAN}$, \mathcal{L}_{color} , and \mathcal{L}_{cyc2} . The loss functions for training D and for training G_1 and G_2 are respectively defined as

$$\begin{aligned}
 \mathcal{L}^D &= \mathcal{L}_{StarGAN}^D(D), \text{ and} \\
 \mathcal{L}^G &= \mathcal{L}_{StarGAN}^G(G_1) + \lambda_{color} \mathcal{L}_{color}(G_2) + \lambda_{cyc2} \mathcal{L}_{cyc2}(G_1, G_2).
 \end{aligned} \tag{9}$$

4 Experiments

4.1 Fine-grained Image Generation.

Experimental Settings. We use the Oxford Flowers dataset [24], which contains 8189 flower images from 102 categories. Each image is annotated with 10 visual descriptions. Following [25], we randomly split the images into 82 seen and 20 unseen categories. To extract the semantic embedding vector of each category, we first extract sentence features from each visual description using the fastText library [26]. Then we average over the features within each category to obtain the per-category feature vector as the semantic embedding. We resize the images to 64×64 as the image size in our experiments. For the SN-GAN part of the model, we use its default hyper-parameters and training configurations. In particular, we train for 200K iterations. For the knowledge part, we use $\lambda_{se} = 0.1$ in our experiments.

Comparing Methods. We compare with SN-GAN trained on the full Oxford Flowers dataset, which potentially represents a performance upper-bound of our method. Besides, we additionally evaluate

Table 1: **Fine-grained Image Generation.** Per-category FID scores of SN-GAN and KG-GANs.

Method	Training data	Condition	\mathcal{L}_{se}	Seen FID	Unseen FID
SN-GAN	$Y_1 \cup Y_2$	One-hot		0.6922	0.6201
One-hot KG-GAN	Y_1	One-hot	✓	0.7077	0.6286
KG-GAN w/o \mathcal{L}_{se}	Y_1	Embedding		0.1412	0.1408
KG-GAN	Y_1	Embedding	✓	0.1385	0.1386

Table 2: **Hair recoloring.** Per-category FID scores of G_1 .

Method	G_1	M	G_2	FID			Average
				Black	Brown	Blond	
StarGAN	✓			1.379	1.287	1.543	1.403
StarGAN + M	✓	✓		1.316	1.236	1.401	1.318
KG-GAN	✓	✓	✓	1.395	1.354	1.530	1.426

two ablations of KG-GAN: (1) One-hot KG-GAN: y is a one-hot vector that represents the target category. (2) KG-GAN w/o \mathcal{L}_{se} : our method without \mathcal{L}_{se} .

Results. To evaluate the quality of the generated images, we compute the FID scores [27] in a per-category manner as in [2]. Then, we average over the FID scores of the set of the seen and the unseen categories, respectively. Table 1 shows the seen and unseen FID scores. We can see from the table that in terms of the category condition, semantic embedding gives better FID scores than one-hot representation. Our full method achieves the best FID scores. For a visual comparison, we show the generated images of two representative unseen categories in Figure 3. As we can see, our full model faithfully generates flowers that have the right color. However, there is room for improvement in terms of the shapes and the structures. It is because color is the major information provided from the visual descriptions of the Oxford Flowers dataset. Also, shapes or structures are more complex to describe than color. For the generated images of the remaining 18 unseen categories, please refer to the supplementary material.

4.2 Hair Recoloring.

Experimental Settings. We use the CelebA dataset [19], which contains 202,599 face images of celebrities. Each image is annotated with 40 binary attributes. We use the three hair attributes (black, brown, and blond) in our experiments. We randomly select 2K images as the test set and use the remaining images as the training set. We center crop the original CelebA images to 178×178 and resize them to 128×128 , which is the image size in our experiments. For the StarGAN part of the model, we use its default hyper-parameters and training configurations except that we set $\lambda_{cls} = 2$. For the knowledge part, We use $\lambda_{color} = 10$ and $\lambda_{cyc2} = 10$ in our experiments.

Evaluation Metrics. We evaluate the realism and the recoloring quality of the generated images. For realism, we use the FID score [27], which is computed from the last convolutional layer features of an Inception-V3 network fine-tuned on the CelebA dataset. For recoloring quality, we measure the segmentation accuracy of the mask network M . To achieve this, we utilize the hair segmentation ground-truth, provided by Borza et al. [28], of 3, 556 images from the CelebA dataset. In particular, we measure three metrics: L1 error, mean squared error (MSE), and MS-SSIM [29].

Realism. We first evaluate the realism of the generated images. Since we do not have any real data as a reference for G_2 , we cannot use FID to evaluate the generated images of G_2 . Therefore, we

Table 3: **Hair recoloring.** Ablation study: segmentation accuracy of the mask network in terms of L1 (smaller is better), MSE (smaller is better), and MS-SSIM (higher is better).

Mask	Generator output	Color loss	Cycle loss	L1	MSE	MS-SSIM
✓	Image	✓		0.1846	0.09922	0.4121
✓	Image	✓	✓	0.1927	0.11350	0.3846
✓	Transformation	✓		0.1439	0.07632	0.5417
✓	Transformation	✓	✓	0.1563	0.07936	0.5361



Figure 4: **Hair recoloring.** Qualitative results of hair segmentation and recoloring with red, green, blue, yellow, cyan, and purple. Please zoom in for better viewing.

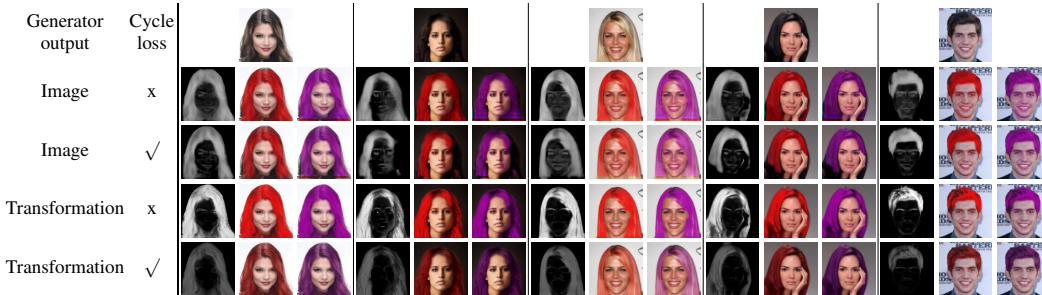


Figure 5: **Hair recoloring.** Visual comparison of the four ablations of our method. The first row shows the input images and each of the remaining rows corresponds to a particular ablation. For each input image and each ablation, we show its segmentation map and two recoloring results.

examine the results of G_2 qualitatively. Figure 4 shows the recoloring results and the corresponding hair segmentation maps. Our G_2 successfully recolors hair into various colors while maintaining its realism (please refer to the supplementary material for more qualitative results).

We still compute FID for G_1 to see whether adding G_2 has any impact on G_1 . Following [2], we compute FID between real and generated images for each category. In particular, we randomly sample 2K images from the training set as the real images and use G_1 to generate 2K fake images of a particular category from the test set. Table 2 shows the FID scores. We can see that: (1) adding mask mechanism improves realism, and (2) the FID scores of G_1 in KG-GAN are worse than those of StarGAN + M . The reason is that our transform generator is more sensitive to the segmentation accuracy than StarGAN’s image generator.

Ablation study. Next, we conduct an ablation study to justify the contributions of each of our proposed components. Note that the mask network and the color loss are necessary components to enable our G_2 . Thus we ablate the generator architecture and the cycle loss. In particular, we evaluate the recoloring quality quantitatively by measuring the segmentation accuracy. As we can see in Table 3, our transform generator significantly outperforms StarGAN’s image generator. We note that the cycle loss greatly improves the realism of G_2 . However, training with cycle loss gives slightly worse segmentation results than without cycle loss. Figure 5 shows a qualitative comparison of our ablated variants. As we can see, adopting our transform generator improves the hair segmentation while adding cycle loss improves realism.

Limitations. Our mask network may recognize eyebrows or beard as hair because their colors are often similar to the hair color. Such false positives do not hurt G_1 but hurt G_2 , because recoloring eyebrows or beard with a bright color is often unrealistic. One possible solution could be teaching M to distinguish hair from eyebrows and beard by collecting an additional category of data whose hair color is uncommon to both eyebrows and beard.

5 Conclusion

We presented KG-GAN, the first framework that incorporates domain-knowledge into the GAN framework for improving diversity. We applied KG-GAN on two tasks to demonstrate its effectiveness. For fine-grained image generation, our results show that when the semantic embedding only provides coarse knowledge about a particular aspect of flowers, the generation of the other aspects mainly borrows from seen classes, meaning that there is still much room for improvement. For hair recoloring, unsupervised segmentation plays an essential role in knowledge. Transformation generator improves segmentation accuracy while cycle-consistency further improves realism. KG-GAN takes the first step towards increasing diversity with knowledge. We hope that our work could inspire future research along the direction of knowledge-guided image generation.

References

- [1] Ian Goodfellow, Jean Pouget-Abadie, Mehdi Mirza, Bing Xu, David Warde-Farley, Sherjil Ozair, Aaron Courville, and Yoshua Bengio. Generative adversarial nets. In *Advances in neural information processing systems*, 2014.
- [2] Takeru Miyato and Masanori Koyama. cgans with projection discriminator. In *ICLR*, 2018.
- [3] Scott Reed, Zeynep Akata, Xinchun Yan, Lajanugen Logeswaran, Bernt Schiele, and Honglak Lee. Generative adversarial text to image synthesis. In *ICML*, 2016.
- [4] Han Zhang, Tao Xu, Hongsheng Li, Shaoting Zhang, Xiaogang Wang, Xiao lei Huang, and Dimitris N Metaxas. Stackgan: Text to photo-realistic image synthesis with stacked generative adversarial networks. In *ICCV*, 2017.
- [5] Phillip Isola, Jun-Yan Zhu, Tinghui Zhou, and Alexei A Efros. Image-to-image translation with conditional adversarial networks. In *CVPR*, 2017.
- [6] Jun-Yan Zhu, Taesung Park, Phillip Isola, and Alexei A Efros. Unpaired image-to-image translation using cycle-consistent adversarial networks. In *ICCV*, 2017.
- [7] Yunjey Choi, Minje Choi, Munyoung Kim, Jung-Woo Ha, Sunghun Kim, and Jaegul Choo. StarGAN: Unified generative adversarial networks for multi-domain image-to-image translation. In *CVPR*, 2018.
- [8] Taesung Park, Ming-Yu Liu, Ting-Chun Wang, and Jun-Yan Zhu. Semantic image synthesis with spatially-adaptive normalization. *arXiv preprint arXiv:1903.07291*, 2019.
- [9] Mehdi Mirza and Simon Osindero. Conditional generative adversarial nets. *arXiv preprint arXiv:1411.1784*, 2014.
- [10] Takeru Miyato, Toshiki Kataoka, Masanori Koyama, and Yuichi Yoshida. Spectral normalization for generative adversarial networks. In *ICLR*, 2018.
- [11] Zhiting Hu, Zichao Yang, Ruslan R Salakhutdinov, LIANHUI Qin, Xiaodan Liang, Haoye Dong, and Eric P Xing. Deep generative models with learnable knowledge constraints. In *Advances in Neural Information Processing Systems*, 2018.
- [12] Ahmed Elgammal, Bingchen Liu, Mohamed Elhoseiny, and Marian Mazzone. CAN: Creative adversarial networks, generating "art" by learning about styles and deviating from style norms. *arXiv preprint arXiv:1706.07068*, 2017.
- [13] Abdullah Hamdi and Bernard Ghanem. IAN: Combining generative adversarial networks for imaginative face generation. *arXiv preprint arXiv:1904.07916*, 2019.
- [14] Qi Mao, Hsin-Ying Lee, Hung-Yu Tseng, Siwei Ma, and Ming-Hsuan Yang. Mode seeking generative adversarial networks for diverse image synthesis. In *CVPR*, 2019.
- [15] Yongqin Xian, Bernt Schiele, and Zeynep Akata. Zero-shot learning - the good, the bad and the ugly. In *CVPR*, 2017.
- [16] Yongqin Xian, Tobias Lorenz, Bernt Schiele, and Zeynep Akata. Feature generating networks for zero-shot learning. In *CVPR*, 2018.
- [17] Rafael Felix, Vijay BG Kumar, Ian Reid, and Gustavo Carneiro. Multi-modal cycle-consistent generalized zero-shot learning. In *ECCV*, 2018.
- [18] Yongqin Xian, Saurabh Sharma, Bernt Schiele, and Zeynep Akata. f-VAEGAN-D2: A feature generating framework for any-shot learning. In *CVPR*, 2019.
- [19] Ziwei Liu, Ping Luo, Xiaogang Wang, and Xiaoou Tang. Deep learning face attributes in the wild. In *ICCV*, 2015.
- [20] Martin Arjovsky, Soumith Chintala, and Léon Bottou. Wasserstein generative adversarial networks. In *ICML*, 2017.
- [21] Ishaan Gulrajani, Faruk Ahmed, Martin Arjovsky, Vincent Dumoulin, and Aaron C Courville. Improved training of wasserstein gans. In *Advances in Neural Information Processing Systems*, 2017.
- [22] Gang Zhang, Meina Kan, Shiguang Shan, and Xilin Chen. Generative adversarial network with spatial attention for face attribute editing. In *ECCV*, 2018.

- [23] Bo Zhao, Bo Chang, Zequn Jie, and Leonid Sigal. Modular generative adversarial networks. In *ECCV*, 2018.
- [24] Maria-Elena Nilsback and Andrew Zisserman. Automated flower classification over a large number of classes. In *ICCVGI*, 2008.
- [25] Scott Reed, Zeynep Akata, Honglak Lee, and Bernt Schiele. Learning deep representations of fine-grained visual descriptions. In *CVPR*, 2016.
- [26] Piotr Bojanowski, Edouard Grave, Armand Joulin, and Tomas Mikolov. Enriching word vectors with subword information. *Transactions of the Association for Computational Linguistics*, 2017.
- [27] Martin Heusel, Hubert Ramsauer, Thomas Unterthiner, Bernhard Nessler, and Sepp Hochreiter. GANs trained by a two time-scale update rule converge to a local Nash equilibrium. In *Advances in Neural Information Processing Systems*, 2017.
- [28] Diana Borza, Tudor Ileni, and Adrian Darabant. A deep learning approach to hair segmentation and color extraction from facial images. In *International Conference on Advanced Concepts for Intelligent Vision Systems*, 2018.
- [29] Zhou Wang, Eero P Simoncelli, and Alan C Bovik. Multiscale structural similarity for image quality assessment. In *The Thrity-Seventh Asilomar Conference on Signals, Systems & Computers, 2003*, 2003.